

Group Velocity Dispersion Management of Microstructure Optical Fibers

S. M. Abdur Razzak, M. A. Rashid, Y. Namihira, and A. Sayeem

Abstract—A simple microstructure optical fiber design based on an octagonal cladding structure is presented for simultaneously controlling dispersion and leakage properties. The finite difference method with anisotropic perfectly matched boundary layer is used to investigate the guiding properties. It is demonstrated that octagonal photonic crystal fibers with four rings can assume negative ultra-flattened dispersion of -19 ± 0.23 ps/nm/km in the wavelength range of $1.275 \mu\text{m}$ to $1.68 \mu\text{m}$, nearly zero ultra-flattened dispersion of 0 ± 0.40 ps/nm/km in a 1.38 to $1.64 \mu\text{m}$, and low confinement losses less than 10^{-3} dB/km in the entire band of interest.

Keywords—Finite difference modeling, group velocity dispersion, optical fiber design, photonic crystal fiber.

I. INTRODUCTION

INDEX guiding microstructure optical fibers (MOFs) or holey fibers [1] usually consist of a hexagonal arrangement of microscopic air-channels running down length of the silica based fiber, surrounding a central solid silica core. Inclusion of air-holes in the cladding creates sufficient index difference between the core and the cladding to guide light by the mechanism of total internal reflection (TIR). One of the appealing characteristics of such fibers is that their dispersion and modal properties can be controlled significantly by varying the size of the air-holes, their number, and their positions. PCFs exhibit a number of unique properties including wide range single mode operation, zero dispersion at visible wavelengths, super high or low nonlinearities, high birefringence, and ultra-flattened dispersion [2]-[5]. Therefore, PCFs are so attractive in controlling application specific dispersion and modal properties.

Control of fiber's chromatic dispersion is crucial for practical applications to optical fiber communication systems, dispersion compensation, and nonlinear optics [3]. Moreover, as there is a finite number of air-holes in the cladding, guided modes of PCF are intrinsically leaky, control of leakage/confinement losses are also crucial. Therefore, the issue of controlling chromatic dispersion keeping confinement

losses to a value below the Raleigh scattering level has witnessed a dramatic growth of efforts over the past years. Various index guiding PCFs with remarkable dispersion and leakage properties [6]-[12], have been reported to date including PCFs design with uniform optimized air-holes [7]-[9], modulating air-holes in radial directions [6, 10, 11], and PCFs with a defected core [12]. Among these designs, since the PCFs in [7]-[9] are not so attractive in the light of confinement loss. These PCFs with small uniform d/Λ require many rings layer to reduce confinement losses below the Raleigh scattering limit. Moreover, adding additional rings to these existing designs in order to reduce the confinement losses may alter both the required dispersion accuracy and nonlinearity. Regarding the PCFs in [6, 10, 11], air-hole modulation show significant reduction in the number of rings but with a consequent increase in number of design parameters. The PCF in [12] require sub micrometer adjustment for the central defect air-hole dimension to ensure dispersion accuracy in flatness. This scenario depicts that still there is rooms to continue efforts to design simple PCF structures for low loss wideband ultra-flattened dispersion.

Beside the hexagonal arrangement of air-holes, other structures such as square [13], octagonal [14], decagonal [15], and circular [16] arrangement of air-holes for PCF have also been proposed. Among these non-hexagonal PCFs, the octagonal PCFs (O-PCFs) are reported to have such attractive features as low confinement losses and inherently high nonlinearity [13, 17] in comparison to hexagonal PCFs. This features of the O-PCFs are explored in this work to design dispersion flattened PCFs.

In this paper, we propose four ring PCF structures that can assume ultra-flattened chromatic dispersion and low confinement losses in a broad range of wavelength. A comparison of the properties of these PCF with some of the remarkable designs [6]-[12] in the light of flat dispersion, low confinement loss, design simplicity is also presented that show novelty of the proposed PCFs. PCFs with such properties as wide band ultra-flattened chromatic dispersion, relatively high nonlinearity, and low confinement losses may pave the way for applications in optical parametric amplification, wavelength conversion, and all optical signal processing.

II. THE PCF MODEL

Fig.1 shows a simple geometry for the proposed dispersion flattened PCFs (hereinafter DF-PCF) with optimized air-hole

S. M. A. Razzak is with the Graduate School of Engineering & Science, University of the Ryukyus, Okinawa 903-0213, Japan (phone: 81-80-31864102; fax: 81-98-8958700; e-mail: razzak91@yahoo.com).

M. A. Rashid is with the Graduate School of Engineering & Science, University of the Ryukyus, Okinawa 903-0213, Japan (e-mail: rashid68@yahoo.com).

Y. Namihira is with the Graduate School of Engineering & Science, University of the Ryukyus, Okinawa 903-0213, Japan.

A. Sayeem is with the Bhulbaria GP School, Natore, Bangladesh.

diameters d_1 , d_2 , and pitch Λ_1 . Since periodicity in the cladding region is not essential to confine the guiding light in the high index core region [10], air-hole diameter on the first ring is scaled down to shape dispersion property while diameter of air-holes on outer rings are kept larger for better field confinement. Pitch Λ_1 is related to Λ_2 by the relation $\Lambda_2 \approx 0.765\Lambda_1$. In contrast to a conventional hexagonal PCF (H-PCF), octagonal PCFs have isosceles triangular unit lattices with a vertex angle of 45°. Due to such lattices, O-PCFs contain more air-holes in the cladding region with the same numbers of rings than H-PCFs. In O-PCFs, the total number of air-holes for rings 1, 2, 3, 4, and 5 are respectively 8, 24, 48, 80, and 120, whereas in a regular triangular lattice, the number of air-holes is 6, 18, 36, 60, and 90, respectively. This results in a higher air-filling ratio and a lower refractive index around the core, thereby providing strong confinement ability. As there are eight air holes on the first ring and is placed in an octagonal rotational symmetry, O-PCF results in similar fundamental field distribution as that of the standard step index fibers [14].

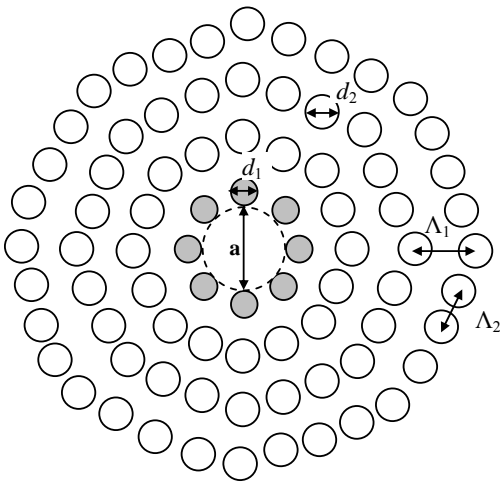


Fig.1 Cross-section of the proposed four rings PCF with air-hole diameters d_1 , d_2 , and pitch Λ_1 .

The following sections present numerical simulation tools and simulation results of this fiber for two different set of optimized parameters.

III. DESIGN METHOD AND EQUATIONS

The computational window was divided by 181 uniform grids in both the x and y axes and was surrounded by 8 PML layers. To model the leakage anisotropic PML layers were used. Once the modal effective index n_{eff} is obtained by solving an eigenvalue problem drawn from the Maxwell equations using the FDM [15, 17], chromatic dispersion D , effective area A_{eff} and confinement loss L_c , can be given by [15] the following equations:

$$D = -\frac{\lambda}{c} \frac{d^2 \text{Re}[n_{eff}]}{d\lambda^2} \quad (1)$$

$$A_{eff} = \frac{[\iint |E|^2 dx dy]^2}{\iint |E|^4 dx dy} \quad (2)$$

$$L_c = 8.686 \times \text{Im}[k_0 n_{eff}] \quad (3)$$

where, $\text{Re}[n_{eff}]$ is the real part of n_{eff} , λ is the wavelength, c is the velocity of light in vacuum, $\text{Im}[n_{eff}]$ is the imaginary part of n_{eff} , and k_0 is the free space wave number. E is the electric field distribution derived by solving an eigenvalue problem drawn from Maxwell's equations. The material dispersion obtained from Sellmeier formula is directly included in the calculation. Hence, D in (1) corresponds to the total dispersion of the PCF.

Using two sets of optimized parameters of the PCF in Fig.1 two dispersion flattened PCFs have been designed. One with negative dispersion-flattened characteristics and another with nearly zero dispersion-flattened characteristics.

A. Negative dispersion-flat PCF

Fig.2 shows wavelength dependence of chromatic dispersion of the proposed negative DF-PCF for optimum design parameters. Optimizing the parameters d_1 , d_2 , and Λ_1 chromatic dispersion of $-19 + 0.230$ ps/nm/km is obtained (dispersion variation 0.23 ps/nm/km) in a wavelength range of 1.275 to 1.68 μm (405 nm) for $\Lambda_1 = 1.70 \mu\text{m}$, $d_1/\Lambda_1 = 0.27$, and $d_2/\Lambda_1 = 0.58$. For optimization of the parameters a simple technique is applied. First a relative air-hole dimension d_2/Λ_1 is chosen in the range of 0.5 to 0.8. Larger value is chosen for better field confinement. Then a value of d_1/Λ_1 is calculated by examining the dispersion curves. Fig. 2 depicts that the octagonal structure is more efficient in tailoring dispersion because modulating only dimension of the first ring it is possible to obtain wideband ultra-flattened dispersion. As a result such PCFs have a modest number of design parameters, two air-hole diameters and a pitch.

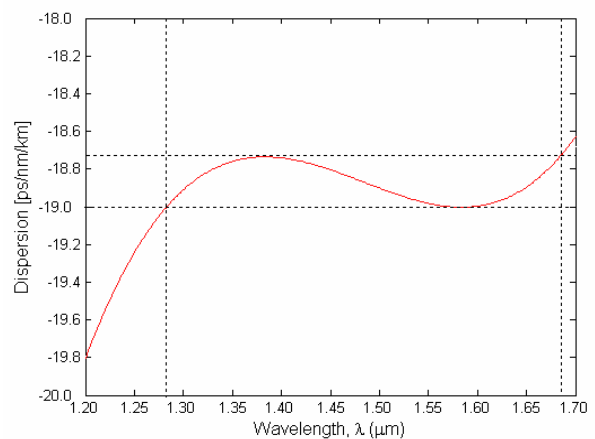


Fig. 2 Optimum dispersion curve of the proposed DF-PCF for $\Lambda_1 = 1.70 \mu\text{m}$, $d_1/\Lambda_1 = 0.27$, and $d_2/\Lambda_1 = 0.58$.

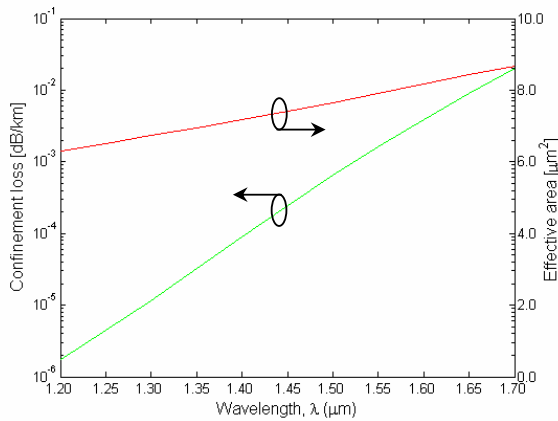


Fig.3 Wavelength dependence of the effective area and confinement losses of the negative DF-PCF for $\Lambda_1 = 1.70 \mu\text{m}$, $d_1/\Lambda_1 = 0.27$, and $d_2/\Lambda_1 = 0.58$.

Moreover such PCFs with only one defected innermost ring can assume relatively smaller effective area than that of the PCFs with two or more defected rings. Fig. 3 shows effective area and confinement loss of the fiber for optimum design parameters. It is clear that effective area at $1.55 \mu\text{m}$ is $7.9 \mu\text{m}^2$ whereas it was $13.2 \mu\text{m}^2$ for the case of H-PCF with two defected rings [6]. The confinement loss is also less than 0.01 dB/km in the entire band of interest. Therefore, we have shown successfully that modulation of air-hole diameter of only the first ring is sufficient to achieve negative ultra-flattened dispersion and low confinement loss in a broad range of wavelengths. Fig. 4 shows optical field intensity of the x polarization component of the guided mode at $1.55 \mu\text{m}$ wavelength. The red color indicates the highest intensity and the blue the lowest. It depicts that the field has confined well within the core. Fibers with such properties as wideband negative dispersion-flattened characteristics, relatively smaller effective area, and low confinement loss may find its way in various nonlinear applications and simultaneously can act as a short length dispersion compensator.

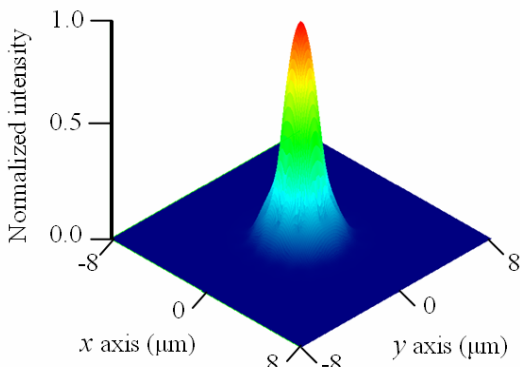


Fig. 4 Mode field profile of the fiber at $1.55 \mu\text{m}$ for $\Lambda_1 = 1.70 \mu\text{m}$, $d_1/\Lambda_1 = 0.27$, and $d_2/\Lambda_1 = 0.58$.

B. Nearly-zero dispersion-flat PCF

Figure 5 shows dispersion characteristic of the DF-PCF for another set of optimized parameters. For the new set : $\Lambda_1 = 2.30 \mu\text{m}$, $d_1/\Lambda_1 = 0.28$, and $d_2/\Lambda_1 = 0.58$; ultra-flattened dispersion curves $0 \pm 0.40 \text{ ps/nm/km}$ is obtained in a 1.38 to $1.64 \mu\text{m}$ (260 nm band centered at $1.55 \mu\text{m}$). The parameters are optimized in a similar way as described in subsection 3.1.

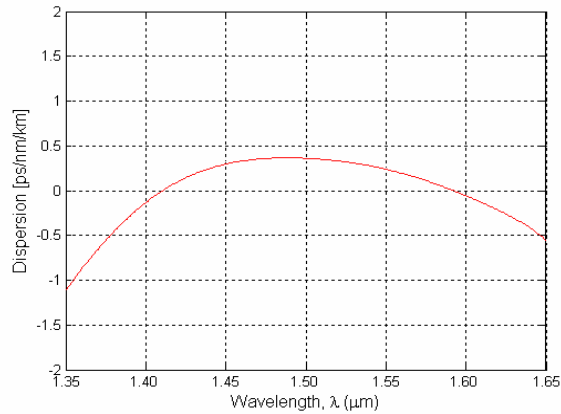


Fig.5 Dispersion characteristics of the DF-PCF for $\Lambda_1 = 2.30 \mu\text{m}$, $d_1/\Lambda_1 = 0.28$, and $d_2/\Lambda_1 = 0.58$.

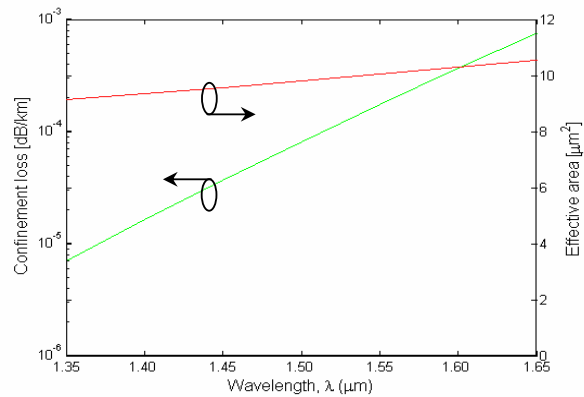


Fig.6 Wavelength dependence of the effective area and confinement losses of the negative DF-PCF for $\Lambda_1 = 2.30 \mu\text{m}$, $d_1/\Lambda_1 = 0.28$, and $d_2/\Lambda_1 = 0.58$.

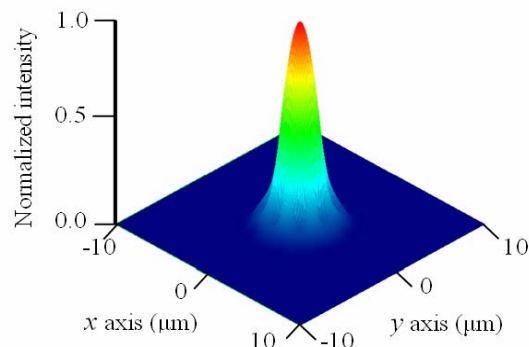


Fig.7 Mode field profile of the fiber at $1.55 \mu\text{m}$ for $\Lambda_1 = 2.30 \mu\text{m}$, $d_1/\Lambda_1 = 0.28$, and $d_2/\Lambda_1 = 0.58$.

Fig.6 shows effective area and confinement loss of the fiber

for the new optimized parameters. Due to increased pitch value effective area this time is relatively larger but still it is less than 10 ($9.6 \mu\text{m}^2$) at $1.55 \mu\text{m}$. The confinement loss is seen to be less than 0.001 dB/km in the entire band of interest. PCFs with such a small group velocity dispersion and negligible third order dispersion can find its way in different applications in nonlinear regimes. Fig. 7 shows optical field intensity of the x polarization component of the guided mode at $1.55 \mu\text{m}$ wavelength. It depicts that the field has confined well within the core.

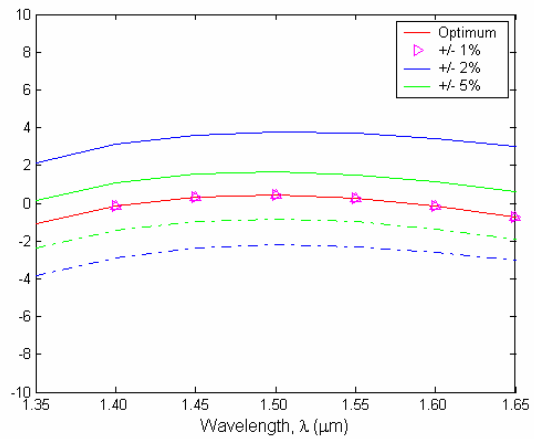
C. Dispersion Tolerance

To study dispersion tolerance of the O-PCFs here we consider a dispersion-flattened case of sub-section 3.2. It is known that in a standard fiber draw, 1% variation in fiber global diameter may occur [9] unavoidably during the fabrication process. It is also reported that dimension of the first ring is particularly important as it affect the dispersion slope significantly [11]. Therefore, roughly an accuracy of 2% may require ensuring required dispersion flatness. To account for this issue air-hole diameters d_1 and d_2 are varied up to $\pm 5\%$ from their optimum values (red lines). Corresponding dispersion curves are shown in Figs. 8(a) and 8(b) respectively. While varying d_1 , d_2 and Λ_1 are kept constant and while varying d_2 , d_1 and Λ_1 are kept constant respectively. It is found that the DF-PCF maintains dispersion flatness within $0 \pm 2.0 \text{ ps}/(\text{nm}\cdot\text{km})$ for diameter variation up to order $\pm 2\%$. Moreover, notice that the dispersion slope characteristics are almost insensitive to incremental variations in the air-hole diameters. Fig. 9 shows dispersion tolerance of the fiber due to changes in the pitch of order $\pm 1, \pm 2$ and $\pm 5\%$ along with the optimum dispersion curve (red line). Fig. 9 ensures that design accuracy of the fiber for incremental change in pitch during the fabrication process is satisfactory as it does not affect the dispersion slope significantly.

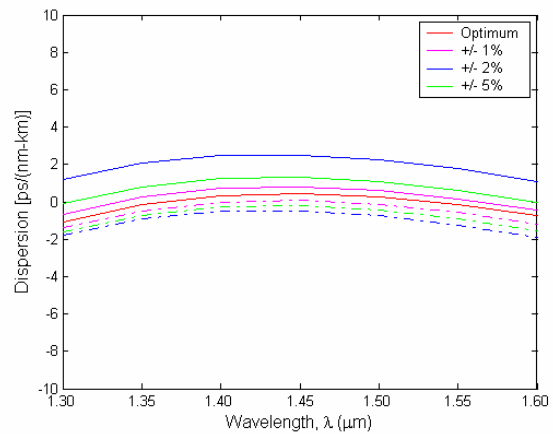
D. Comparison between DF-PCFs and Existing PCF Designs Negative

Table 1 compares DF-PCFs properties and some other existing designs for ultra-flattened PCFs in the references considering the ultra-flattened dispersion range, confinement loss, and number of design parameters including the number of air-hole ring layers. N_r , N_Λ , and N_d correspond to the number of rings, pitches, and air-hole diameters used in PCF design, respectively. Note that PCFs in [7] to [9] need many rings to reduce the confinement losses. Although PCF in [12] is attractive in the light of the abovementioned properties, its dispersion accuracy is supposed to be low because of the central defect air-hole in the core. On the other hand, the proposed DF-PCFs has ultra-flattened chromatic dispersion in the C band, low confinement loss, and less design complexity, i.e., fewer design parameters as well as better fabrication tolerance to parameter variations as is demonstrated in section 4. From the above scenario we hope that octagonal structure based dispersion-flattened fibers can be very good alternatives

to the conventional PCFs especially in the light of dispersion tolerance, confinement losses, and number of design parameters.



(a)



(b)

Fig. 8 Dispersion tolerance of the DF-PCF: (a) optimum dispersion and effects of variation in d_1 , (b) optimum dispersion and effects of variation in d_2 .

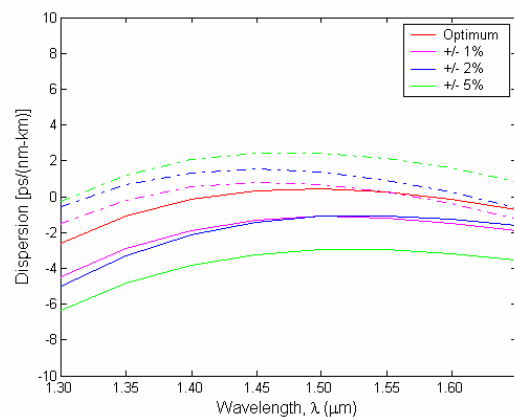


Fig. 9 Dispersion properties of the DF-PCF for pitch variation of order 1 to $\pm 5\%$ around the optimum value (red line).

TABLE 1 COMPARISON OF DF-OPCF PROPERTIES WITH SOME REMARKABLE DESIGNS

PCFs Design	ΔD ps/nm/km	L_c dB/km	1FDR (nm)	2NDP (N_r, N_d, N_λ)
Ref. [6]	0.50	-	430	4, 1, 2
Ref. [10]	0.80	< 0.1	490	4, 1, 4
Ref. [11]	0.20	0.016	100	4, 1, 4/5
Ref. [12]	0.40	0.013	506	4, 1, 2
DF-PCF	0.46/ 0.80	< 0.01/ 0.001	405/ 260	4, 1, 2

1FDR - flat dispersion range, 2NDP -number of design parameters,

IV. CONCLUSION

Two different cases of dispersion-flattened octagonal PCFs have been discussed with numerical simulation results. Dispersion tolerance and comparison with other existing PCFs design are also compared in the light of flattened dispersion, confinement loss, and design complexity. It has been demonstrated that octagonal photonic crystal fibers with four rings can assume negative ultra-flattened dispersion of $-19 + 0.23$ ps/nm/km in the wavelength range of $1.275 \mu\text{m}$ to $1.68 \mu\text{m}$, and nearly zero ultra-flattened dispersion of 0 ± 0.40 ps/nm/km in a 1.38 to $1.64 \mu\text{m}$ with low confinement losses less than 10^{-3} dB/km in the entire band of interest.

REFERENCES

- [1] J. C. Knight, T. A. Birks, P. St. J. Russell, and D. M. Atkin: "All-silica single-mode optical fiber with photonic crystal cladding," Opt. Lett., Vol. 21, pp.1547-1549 Oct. 1996.
- [2] T. Matsui, J. Zhou, K. Nakajima, and I. Sankawa, "Dispersion-flattened Photonic Crystal Fiber with Large Effective area and Low Confinement Loss," J. Lightwave Technology, Vol. 23, No. 12, pp. 4178-4183, Dec 2005.
- [3] K. Saitoh and M. Koshiba, "Highly nonlinear dispersion-flattened photonic crystal fibers for supercontinuum generation in the telecommunication window," Opt. Express, Vol. 12, No. 10, pp. 2027-2032, May 2004.
- [4] T. Okuno et al, "Highly nonlinear and perfectly dispersion flattened fibers for efficient optical signal processing application," Electron. Lett. Vol. 39, pp. 972, 2003.
- [5] K. P. Hansen, "Dispersion flattened hybrid-core nonlinear photonic crystal fiber," Opt. Express, Vol. 11, No. 13, pp. 1503-1509, June 2003.
- [6] T. L. Wu and C. H. Chao, "A novel ultraflattened dispersion photonic crystal fiber," IEEE. Photon. Technol. Lett. 17, 67-69, 2005.
- [7] A. Ferrando, E. Silvestre, P. Andres, J. J. Miret, and M. Andres: "Nearly zero ultraflattened dispersion in photonic crystal fibers," Opt. Lett. Vol. 25, No. 11, pp. 790-792, June 2000
- [8] A. Ferrando, E. Silvestre, P. Andres, J. Miret, and M. Andres: "Designing the properties of dispersion-flattened photonic crystal fibers," Opt. Express, Vol. 9, No. 13, pp. 687-697, Dec. 2001
- [9] W. H. Reeves, J. C. Knight, and P. St. J. Russell: "Demonstration of ultra-flattened dispersion in photonic crystal fibers," Opt. Express, Vol. 10, No. 14, pp. 609-613, 2002
- [10] K. Saitoh, M. Koshiba, T. Hasegawa, and E. Sasaoka: "Chromatic dispersion control in photonic crystal fibers: application to ultra flattened dispersion," Opt. Express, Vol. 11, pp. 843-852, May 2003
- [11] F. Poletti, V. Finazzi, T. M. Monro, N.G.R. Broderick, V. Tse, and D.J. Richardson, "Inverse design and fabrication tolerances of ultra-flattened dispersion holey fibers," Optics Express 13, No. 10, pp. 3728-3736, May 2005.
- [12] K. Saitoh, N. J. Florous, and M. Koshiba: "Ultra-flattened chromatic dispersion controllability using a defect-core photonic crystal fiber with low confinement loss," Optics Express, Vol. 13, No. 21, pp. 8365-8371, 2005
- [13] A.H. Bouk, A. Cucinotta, F. Poli, S. Selleri, "Dispersion properties of square lattice photonic crystal fibers," Opt. Express Vol. 12, pp.941-946, March 2004.
- [14] Jung-Sheng Chiang and Tzong-Lin Wu: "Analysis of propagation characteristics for an octagonal photonic crystal fiber (O-PCF)," Opt. Comm. Vol. 258, issue-2, pp. 170-176, Feb. 2006
- [15] S. M. Abdur Razzak, Y. Namihira, F. Begum, S. Kaijage, N. H. Hai, and Z. Zou, "Design of a decagonal photonic crystal fiber for ultra-flattened chromatic dispersion," IEICE Trans. Electron., vol. E90-C, no.11, pp. 2141-2145, Nov. 2007.
- [16] Alexander Argyros, Ian M. Bassett, Martijn A. van Eijkelenborg, Maryanne C.J. Large and Joseph Zagari, "Ring structures in microstructured polymer optical fibers" Optics Express, Vol. 9, No. 13, pp813-820, December 2001.
- [17] K. Kaneshima, Y. Namihira, N. Zou, H. Higa, and Y. Nagata: "Numerical investigation of octagonal photonic crystal fibers with strong confinement field", J. IEICE, vol. E89-C, No. 6, pp. 830-837, (2006)